*Tectonophysics*, 168 (1989) 283–296
Elsevier Science Publishers B.V., Amsterdam – Printed in The Netherlands



# Comparison of fluid inclusion decrepitation and acoustic emission profiles of Westerly granite and Sioux quartzite

DONALD L. HALL * and ROBERT J. BODNAR **

*Department of Geological Sciences, Virginia Polytechnic Institute and State University, Blacksburg, VA 24061 (U.S.A.)*

(Received August 11, 1988; revised version accepted February 9, 1989)

## Abstract

Hall, D.L. and Bodnar, R.J., 1989. Comparison of fluid inclusion decrepitation and acoustic emission profiles of Westerly granite and Sioux quartzite. *Tectonophysics*, 168: 283–296.

Acoustic emissions recorded during slow heating of rocks at 1 atm have generally been attributed to intergranular stresses generated by differences in thermal expansion coefficients and elastic moduli of neighboring grains. These experiments have considered only the solid phases in analysis of the results, and little attention has been given to the role of intragranular or grain boundary fluid inclusions in initiating or facilitating fracturing.

In principle, fluid inclusions may be thought of as a special case in which the "neighboring grains" are fluids rather than the usual solid mineral phases. The major differences are that (1) the number of inclusions per unit volume is usually $10^2$ to $10^6$ times greater than the number of mineral grains in that same volume and that (2) the volume increase with temperature for most fluids is 1–2 orders of magnitude greater than for minerals. Thus, when fluid inclusion "grains" are considered, the absolute number of grain-to-grain contacts in a given sample volume is several orders of magnitude greater than if the inclusions are not considered. Further, the magnitude of the stresses between any two adjacent grains may be much higher if one of the "grains" is a fluid inclusion, owing to the larger coefficient of thermal expansion of the fluid relative to a solid phase. As a result, substantial overpressures may be generated at the fluid inclusion "grain"–mineral grain contact, during heating experiments. These overpressures result in brittle failure when the stress around the inclusion exceeds the local strength of the host crystal. In fluid inclusion terminology, this fracturing event is referred to as decrepitation.

Samples of Westerly granite and Sioux quartzite were heated at 2° C/min in a gas-flow stage in order to determine the decrepitation profiles (number of decrepitations as a function of temperature) of these rocks. Decrepitation was monitored visually during heating experiments, and was evidenced by the explosive loss of fluids from the inclusion during a fracturing event. Decrepitation produces microfractures which originate at decrepitated fluid inclusions and propagate outward into the surrounding mineral. Four different types of inclusions, based on room temperature phase ratios and distribution within the host phase, were noted in Westerly granite. Type (1) inclusions contain a single aqueous liquid, type (2) are two-phase, liquid-rich inclusions, type (3) are mostly one-phase fluid inclusions that occur in dense clusters in plagioclase and type (4) are two-phase, moderate-density, $H_2O$–$CO_2$–"salt" inclusions. Type (5) inclusions are one-phase, aqueous liquid inclusions observed in Sioux quartzite.

Fluid inclusions in Westerly granite decrepitate between 75° and 573° C with peaks at 275–300° C and 400–450° C. Type (4) inclusions in Westerly granite tend to decrepitate at lower temperatures (75–300° C) than other inclusion types. Initial fracturing of the quartz host surrounding type (1) inclusions (primary decrepitation) generally occurs over the range 100–400° C and the fractures continue to propogate through the quartz (secondary decrepitation) during further heating from 400° to 573° C. Fluid inclusions in Sioux quartzite decrepitate between 188° and 573° C with a broad maximum at 250–450° C. Primary decrepitation generally occurs at 200–450° C while secondary decrepitation occurs at 350–573° C in Sioux quartzite. Some small inclusions in both samples do not decrepitate until the quartz $\alpha$–$\beta$ transition temperature (573° C) is reached.

* Present address: Department of Earth Sciences, University of California, Riverside, CA 92521 (U.S.A.).

** Person to whom correspondence should be addressed.

0040-1951/89/$03.50 

Decrepitation profiles determined in this study display many similarities and differences when compared to previously published acoustic emission profiles of Westerly granite and Sioux quartzite. Owing to fundamental differences in the techniques used to measure acoustic emission and decrepitation, and the potentially different energies associated with the two events, it is unclear whether decrepitating fluid inclusions are recorded during acoustic emission studies. However, if decrepitating fluid inclusions are being recorded during acoustic emission measurements, then our results suggest that: (1) decrepitation contributes more to low temperature portions of acoustic emission profiles than to high temperature portions for both Sioux quartzite and Westerly granite; (2) compared to Westerly granite, a larger percentage of acoustic emissions in the low temperature decrepitation profile of Sioux quartzite is due to fluid inclusions; (3) decrepitating fluid inclusions, not stresses generated by solid–solid interactions, cause the majority of intragranular fracturing in quartz below the temperature of the $\alpha$–$\beta$ transition in both these rocks.

## Introduction

Many recent studies have examined the effects of temperature and pressure on mechanical and transport properties of rocks. The investigations have shown that elastic moduli (Heard and Page, 1982; Wang and Heard, 1985), coefficients of thermal expansion (Wong and Brace, 1979; Heard, 1980), fracture toughness (Meredith and Atkinson, 1985), thermal conductivity (Walsh and Decker, 1966; Durham and Abey, 1981), porosity (Johnson et al., 1978; Simmons and Cooper, 1978), permeability (Potter, 1978; Summers et al., 1978; Morrow et al., 1981; Trimmer et al., 1980), electrical properties (Olhoeft, 1981) and seismic velocities (Hadley, 1976; Johnson et al., 1978) change when rocks are subjected to elevated temperatures and pressures, and that many of these changes are directly related to the initiation and propagation of microfractures within the rock. In some studies acoustic emissions have been used to monitor microfracturing in rocks and to provide an estimate of the relative importance of microfracturing over a given temperature interval (Johnson et al., 1978; Bauer and Johnson, 1979; Kurita and Fujii, 1979; Yong and Wang, 1980; Atkinson et al., 1984; Carlson et al., 1986; Wang et al., 1989). *In these studies it is generally assumed that acoustic emissions result solely from grain boundary and intragranular cracking due to intergranular stresses, which in turn result from thermal expansion anisotropy and/or mismatch between neighboring grains.*

In fluid inclusion studies a similar technique, decrepitometry, has been used to gain information on large populations of fluid inclusions in rocks (Scott, 1948; Roedder, 1984; Hladky and Wilkins, 1987; Burlinson, 1989). With this technique, mineral samples (usually crushed to sand-sized grains) are subjected to a slow, uniform temperature increase at atmospheric pressure, and decrepitation events are recorded by a sensitive microphone or acoustic transducer. Decrepitations are attributed to fracturing of the mineral surrounding fluid inclusions, which occurs when the fluid pressure in an inclusion exceeds the local strength of the host crystal. Decrepitometry has been applied successfully in mineral exploration to identify favorable inclusion types and to distinguish between mineralized and barren veins (e.g., Burlinson et al., 1983; see also Roedder, 1984).

Recent studies have attempted to correlate the temperatures of homogenization ($T_h$) and decrepitation ($T_d$) by visually monitoring the samples during heating (Bodnar and Bethke, 1984; Bodnar et al., 1989; Ulrich and Bodnar, 1988). In these studies, a doubly polished section of the rock or a cleavage fragment of a mineral is used in place of the crushed samples commonly used in decrepitation analyses, and $T_h$ and $T_d$ are recorded as the sample is heated. In general, these studies show that there is no simple relationship between $T_h$ and $T_d$ (or the formation temperature) as some earlier workers had assumed. These incorrect assumptions resulted in errors in homogenization or trapping temperatures of the fluid inclusions deduced from decrepitation data (e.g., Peach, 1949; Smith, 1950; see also discussion in Bodnar et al., 1989).

All minerals and rocks contain fluid inclusions, in quantities ranging from $\sim 10^2$ to $10^9$ inclusions per cubic centimeter (Roedder, 1984). It is also known that, when these rock or mineral samples are heated, the inclusions will decrepitate. Further, decrepitation releases energy in the form of sound—this is the principle upon which fluid

inclusion decrepitometry is based—and produces fractures in the mineral sample. These same phenomena, that is, the release of energy during heating and the generation of microfractures in the sample, are also characteristic of acoustic emission studies of natural rock and mineral samples. The obvious questions then are whether the two techniques are actually measuring the same phenomena and, if so, what are the relative contributions of solid–solid interactions and fluid–solid interactions to acoustic emission and decrepitation profiles. We have begun a research effort in an attempt to answer this question. In this communication we present the initial results of this effort and compare the acoustic emission and decrepitation profiles of Westerly granite and Sioux quartzite—two very important rock types which have been the focus of numerous past investigations of rock mechanical properties.

## Background

Acoustic emission studies have been conducted by many workers in an effort to understand variations in mechanical properties of rocks and minerals at various temperature and pressure conditions. Energy released and recorded during slow heating of rocks at 1 atm has generally been attributed to fracturing related to intergranular stresses generated by differences in thermal expansion coefficients and elastic moduli of neighboring grains. Workers have in the past considered only the sample mineralogy in analysis of the results, and little attention has been given to the role of intragranular or grain boundary fluid inclusions in initiating or facilitating fracturing to produce "acoustic emissions".

In principle, fluid inclusions may be thought of as a special case in which the "neighboring grains" in a sample are fluids rather than the usual solid mineral phases, and the same rules used to analyze solid–solid interactions will apply in interpretation of the data. The major differences are that the number of inclusions per unit volume is usually $10^2$ to $10^6$ times greater than the number of mineral grains in that same volume of rock (Roedder, 1984), and that the volume increase with temperature for most fluids in 1–2 orders of magnitude greater than for minerals (Fig. 1). Thus, when fluid inclusion "grains" are considered, the absolute number of grain-to-grain contacts in a given sample volume is several orders of magnitude greater than if the inclusions are not considered. Further, the magnitude of the stresses between any two adjacent grains may be much higher if one of the "grains" is a fluid inclusion, owing to the larger coefficient of thermal expansion of the fluid relative to a solid phase. Figure 1 compares the percent volume change of water to that of quartz as a function of temperature at pressures of 1, 3 and 5 kbar. In all cases, during heating the volume percent expansion of water is 1–2 orders of magnitude greater than quartz, and is most pronounced at lower pressures and higher temperatures. As a result of the large coefficient of thermal expansion of the fluid relative to the mineral host, substantial overpressures may be generated in the fluid inclusions or, more precisely, at the inclusion "grain"–mineral grain contact, during heating experiments. These overpressures result in brittle failure when the stress around the fluid inclusion exceeds the local strength of the host crystal. In fluid inclusion terminology, this fracturing event is referred to as decrepitation.

Decrepitation occurs when the pressure inside of a fluid inclusion becomes sufficiently high to cause the mineral surrounding the inclusion to fracture. Figure 2 shows a schematic $P$–$T$ projection of the liquid–vapor curve for a one-compo-

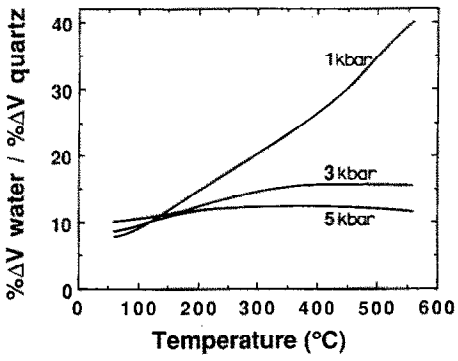


Fig. 1. Percent volume change of water divided by the percent volume change of quartz as a function of temperature at 1, 3 and 5 kbar. Volume changes are referenced to the specific volumes of these phases at 20 °C and $P$. Data for water from Burnham et al. (1969). Data for quartz from Birch (1966), Skinner (1966), and Koster Van Groos and Ter Heege (1973).

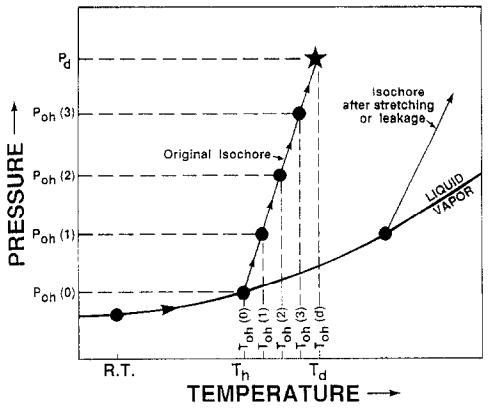


Fig. 2. Schematic pressure–temperature projection of the liquid–vapor curve for a one component fluid illustrating the decrepitation behavior of a given fluid inclusion and the heating procedure used for collection of decrepitation data. Arrows show the path followed by the inclusion during heating. See text for discussion.

nent fluid (e.g., $H_2O$, $CO_2$, $CH_4$) and the path followed by a liquid-rich inclusion when heated from room temperature (R.T.), through the initial homogenization temperature ($T_h$), and finally to the decrepitation temperature ($T_d$). Below the homogenization temperature, vapor pressures are low (e.g., $< 220$ bar for pure $H_2O$; $< 74$ bar for pure $CO_2$; $< 46$ bar for pure $CH_4$) and the pressure increases slowly with increasing temperature. Once the inclusion homogenizes to the liquid phase ($T_h$, Fig. 2), the inclusion follows the isochore, or constant volume line corresponding to its bulk density, with continued heating and the pressure inside the inclusion increases rapidly. At some temperature ($T_d$) above $T_h$ the internal pressure ($P_d$) becomes sufficiently high to cause the fluid inclusion to decrepitate (Fig. 2). For simplicity, the term "decrepitation" will be used to describe all types of non-elastic deformation experienced by fluid inclusions in this study. The mechanism of deformation of quartz is thought to be microfracturing in all cases, although other mechanisms have been proposed for weaker minerals such as fluorite and barite. The interested reader is referred to Bodnar and Bethke (1984, pp. 150–154) for a detailed discussion of the various types of deformation (e.g. stretching, leakage, partial decrepitation) commonly associated with fluid inclusions, and the terminology proposed to describe this deformation.

Several factors are known to influence the 1 atm decrepitation behavior of fluid inclusions. It is evident from Fig. 2 that the homogenization temperature ($T_h$), or density, exerts a fundamental control over the decrepitation temperature ($T_d$) of a group of isocompositional fluid inclusions. Inclusions having lower $T_h$ (i.e., higher density) tend to decrepitate at lower temperatures than similar composition inclusions that have higher $T_h$, or lower density. The slope of the isochore in $P$–$T$ space, which is directly related to the density and composition of the inclusion, also controls $T_d$. Inclusions with steep isochores tend to decrepitate at lower temperatures than those with less steep isochores. Numerous studies have shown that $T_d$ is related to host-mineral properties, especially Moh's hardness (Tugarinov and Naumov, 1970; Poland, 1982). Fluid inclusions in soft minerals such as barite decrepitate with only a few ten's of bars of internal pressure (Ulrich and Bodnar, 1988), while fluid inclusions in harder minerals such as quartz can withstand up to a few kilobars of internal pressure before decrepitation begins (Gratier and Jenatton, 1984; Bodnar et al., 1989). These studies have also shown that small inclusions can sustain larger internal pressures compared to large inclusions with the same $T_h$ and composition (Leroy, 1979; Bodnar et al., 1989). Inclusion shape has a minor influence on $T_d$, with more regularly shaped fluid inclusions able to withstand slightly higher internal pressures than irregularly shaped inclusions (Bodnar et al., 1989). The effect of time on $T_d$ is presently unknown but is thought to be relatively unimportant during 1 atm. decrepitation studies (Bodnar et al., 1989).

## Methodology

The sample of Westerly granite used in this study was an approximately 3 cm × 4 cm × 2 cm block taken from the same sample as was used by Carlson et al. (1986) in their study of thermal cracking in Westerly granite. The sample of Sioux quartzite used in this study was a cylindrical core,

2 cm in diameter and 4 cm in length taken from the same block as the samples used by Friedman and Bur (1974) in their study of residual strain, fabric, fracture, and ultrasonic attenuation and velocity, and by Friedman and Johnson (1978) in their study of thermal cracking. Several doubly polished thin sections approximately 100–200 $\mu$m thick were prepared from these samples using standard techniques (Roedder, 1984). Decrepitation data were collected by slowly heating (2°C/min) preselected fluid inclusions in a FLUID INC-adapted U.S. Geological Survey gas-flow heating/freezing stage (Werre et al., 1979). Approximately 200 inclusions were studied for each sample. Decrepitation events were recorded by visually monitoring fluid inclusions with a petrographic microscope and recording as the decrepitation temperature the temperature at which the inclusion exploded, or experienced an increase in $T_h$ as explained below.

The inclusion subpopulations were chosen to be representative of the total inclusion population in terms of relative abundance of the various inclusion types. There is some bias in these subpopulations however, due to the limits of optical resolution which excluded most inclusions less than 1–2 $\mu$m, including all those in plagioclase, from the test populations. A summary of data collected during this study is provided in Table 1.

The homogenization temperature ($T_h$, Fig. 2) of each two-phase (liquid + vapor) fluid inclusion in the test populations was measured and recorded. Inclusions were then heated to temperatures above $T_h$ in increments of 10–25°C ($T_{oh}(1)$, $T_{oh}(2)$, etc, Fig. 2). After each heating increment the sample was slowly cooled and $T_h$ remeasured. If $T_h$ remained the same within experimental precision ($\pm 1.0$°C), the inclusion was assumed to have behaved elastically during heating. If $T_h$ increased during the heating increment it was assumed that the inclusion decrepitated ($T_d$, Fig. 2). Many of the inclusions in Westerly granite, and nearly all fluid inclusions in Sioux quartzite, are one-phase aqueous inclusions at room temperature. Vapor bubbles could not be nucleated in the single-phase inclusions, even on cooling to $-196$°C with liquid nitrogen. Hence, the initial $T_h$ was not measurable for one-phase fluid inclusions and decrepitation could not be determined by monitoring changes in $T_h$. Instead, $T_d$ was defined as the heating increment that caused a vapor bubble to nucleate on cooling the inclusion to room temperature. The unavoidable assumption in this definition is that when the inclusion partially decrepitates the volume increase is sufficient to render the inclusion two-phase at room temperature. This approximation would overestimate the strength of these inclusions slightly (i.e., overestimate $T_d$) if the inclusions remain one phase fluids after partial decrepitation. However, most inclusions are unlikely to remain single-phase after partial decrepitation as the volume increase, or loss of fluid from the inclusion, at elevated temperature is usually sufficient to produce a vapor bubble during subsequent cooling of the sample to room temperature.

Fluid inclusions observed during this study often experienced incremental increases in $T_h$ on heating to temperatures above $T_d$, presumably re-

TABLE 1

Summary of homogenization ($T_h$) and decrepitation ($T_d$) data

| Inclusion type [a]: | 1 | 2 | 3 | 4 | 5 |
|---|---|---|---|---|---|
| Average $T_h$ | nm | nm | 185 | 320 [b] | nm |
| Range in $T_h$ | nm | nm | 175–200 | 310–330 | nm |
| Average $T_d$ | 261 (479) | nm | 288 | 212 | 321 (439) |
| Range in $T_d$ | 75–388 (413–573) | nm | 165–385 | 78–350 | 188–573 (313–573) |
| Number of observations | 75 (77) | nm | 18 | 42 | 142 (61) |

[a] Inclusion types: (1) one-phase, NaCl–$CaCl_2$–$H_2O$, Westerly; (2) one-phase, in plagioclase, Westerly; (3) two-phase, low salinity, Westerly; (4) $CO_2$–$H_2O$–"salt", Westerly; (5) one phase, NaCl–$H_2O$, Sioux.

[b] Only measured for inclusions that did not decrepitate before Th. nm: not measured; between parentheses: data from secondary decrepitations.

sulting from stepwise propagation of microfractures, although this has not been verified. Similar stepwise increases in $T_h$ were observed by Bodnar et al. (1989) in their study of the decrepitation behavior of inclusions in quartz. In the present study, the internal pressures necessary to cause subsequent incremental decrepitation events, roughly estimated to be 0.5–1.5 kbar, is generally much lower than the initial decrepitation pressure of 2–3 kbar (for 2–5 $\mu$m inclusions; see Bodnar et al., 1989). This is to be expected because the critical stress necessary to propagate a microfracture is usually less than that required to initiate it, especially when an aqueous phase (e.g. a fluid inclusion) is present to hydrolytically weaken the crack tip (Atkinson, 1984; Dunning et al., 1984; Swanson, 1984). Incremental decrepitation generally culminates in complete decrepitation whereby the fluid inclusion loses all of its contents. For each inclusion, we refer to the first detected volume increase as the primary decrepitation, and all subsequent events recorded for the same inclusion are designated as secondary decrepitations.

## Fluid inclusion petrography

Four types of fluid inclusions occur in Westerly granite. The most common, type (1), lie along healed, subparallel intragranular microfractures in quartz and average 2–3 $\mu$m in maximum dimension (Fig. 3A). These contain a one-phase liquid at room temperature with a eutectic temperature ($T_e$) of approximately $-52\,^\circ$C and a final melting point of ice ($T_m$ ice) of approximately $-10\,^\circ$C. No vapor bubble was present initially in these inclusions and, because vapor-absent phase transitions at low temperatures are generally metastable (Roedder, 1984), $T_e$ and $T_m$ ice were measured from partially decrepitated or stretched fluid inclusions that had nucleated a vapor bubble on cooling. Microthermometric data suggest that the fluid is dominantly $NaCl-CaCl_2-H_2O$ with a salinity of about 14 wt.% NaCl equivalent.

Type (2) fluid inclusions generally occur in dense clusters in the cores of plagioclase crystals (Fig. 3B), but also occur along healed, intragranular fractures in plagioclase and microcline. These fluid inclusions are so abundant in places that they resemble sericitic alteration when the sample is observed at low magnification. However, when observed at high power under oil immersion (Fig. 3C) these areas are resolved into dense patches of mostly one-phase, liquid inclusions; this identification was confirmed by SEM observations (Fig. 4A, D). None of these inclusions was large enough to monitor during heating tests.

Type (3) inclusions occur along healed, intragranular microfractures in quartz (Fig. 3D), similar to the occurrence of type (1) inclusions. They differ from type (1), however, in that they are slightly larger ($\sim 5$ $\mu$m), consist of two fluid phases (liquid + vapor) at room temperature and contain nearly pure $H_2O$ ($T_m$ ice of $0\,^\circ$ to $-1\,^\circ$C). These fluid inclusions display homogenization temperatures of 175–200 °C.

Type (4) inclusions in Westerly granite contain aqueous solution, liquid $CO_2$ and $CO_2$ vapor at room temperature and occur as isolated inclusions

Fig. 3. Examples of fluid inclusions in Westerly granite and Sioux quartzite. Scale bar is 25 $\mu$m in length in all photographs. Photos A and C were taken in plane-polarized light under oil immersion; all others were taken in plane-polarized light in air. A. One-phase (liquid) fluid inclusions in Westerly granite along healed, intragranular fractures in quartz. B. Dense cluster of fluid inclusions in Westerly granite in the core of a plagioclase crystal. Most inclusions consist of a one-phase liquid. C. Higher magnification view of portion of plagioclase crystal in B showing individual one-phase (liquid) fluid inclusions that comprise the dense cluster. D. Two-phase (liquid + vapor) fluid inclusions in Westerly granite along a healed, intragranular fracture in quartz. E. Randomly oriented fluid inclusions in quartz from Westerly granite containing $H_2O-CO_2$–"salt". The photograph was taken at $T > T_h$ $CO_2$; therefore, the phases present are saltwater and liquid $CO_2$. F. Irregular patch of one-phase (liquid) fluid inclusions in quartz from Sioux quartzite. G. One-phase (liquid) fluid inclusions in Sioux quartzite along healed, intragranular fractures in quartz. H. Decrepitated $H_2O-CO_2$–"salt" fluid inclusion in quartz from Westerly granite displaying a large microfracture. This inclusion decrepitated at 320 °C, prior to homogenization. I. Oriented microfracture array developed in Sioux quartzite. Many of the microfractures can be traced to individual fluid inclusions. This sample was heated to 500 °C. J. One-phase (liquid) fluid inclusions in Sioux quartzite along original quartz grain boundaries separating original grains and quartz overgrowths.

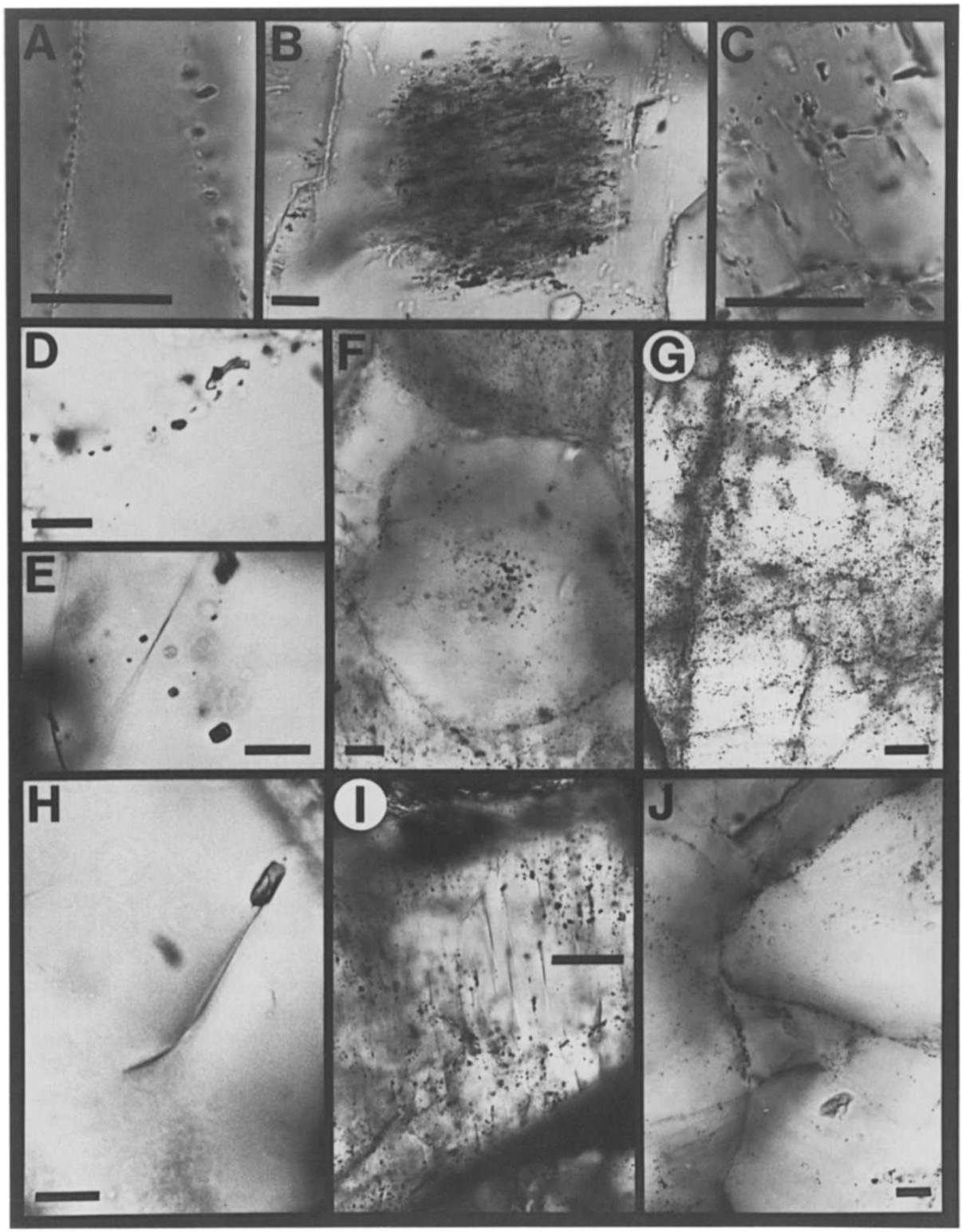
A
B
C
D
F
G
E
H
I
J

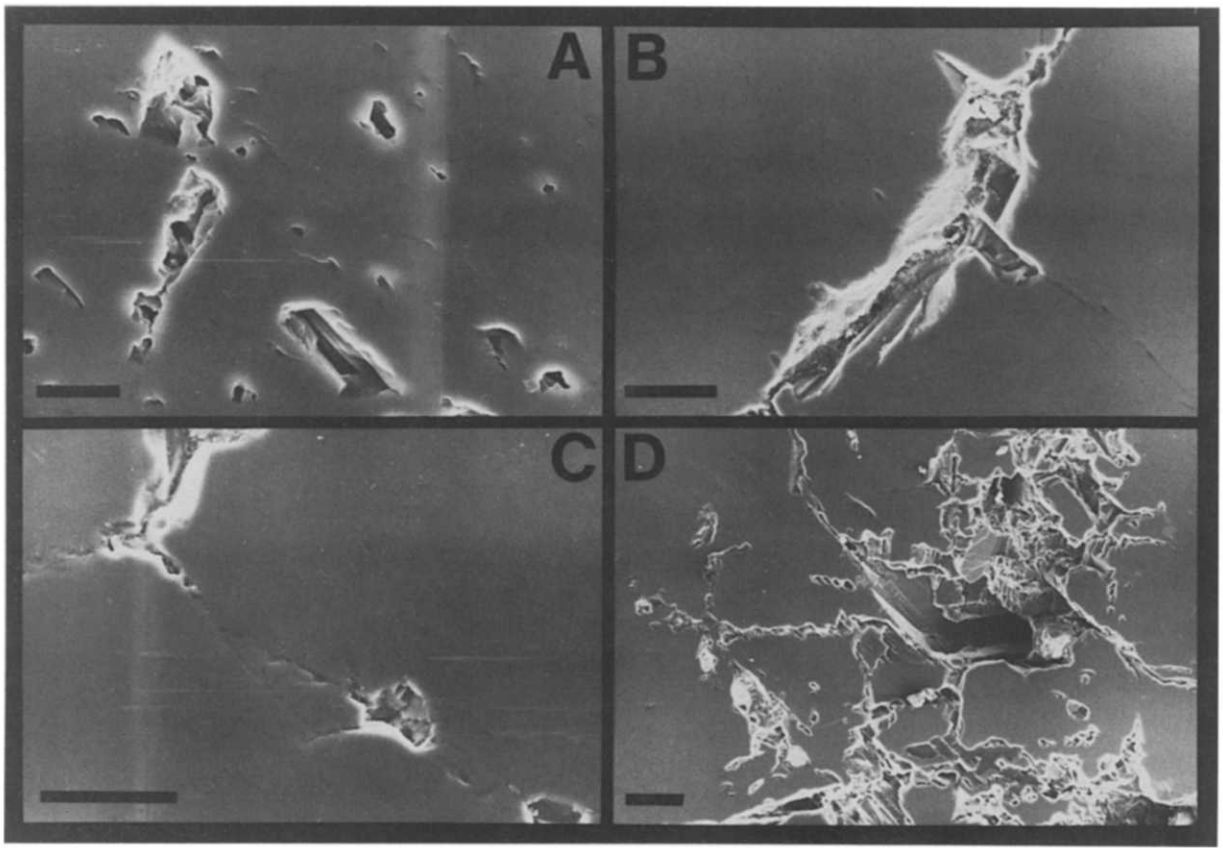


Fig. 4. Scanning electron photomicrographs of exposed fluid inclusions in Westerly granite and Sioux quartzite. Scale bar is 10 $\mu$m in length in A and 25 $\mu$m in length in B–D. A. Fluid inclusions in plagioclase in Westerly granite (unheated). B. Decrepitated fluid inclusions in quartz along healed, intragranular fracture in Westerly granite showing short microfractures oriented approximately perpendicular to the healed, microfracture. This sample was heated to 500 °C. C. Decrepitated fluid inclusions along healed intragranular fracture in quartz from Sioux quartzite. This sample was heated to 550 °C. D. Decrepitated fluid inclusions in plagioclase in Westerly granite showing microfracturing and disaggregation as a result of heating to 550 °C.

or in small groups (Fig. 3E). Melting temperatures of $CO_2$ are $\approx -57$ °C and $CO_2$ liquid-vapor homogenization to the liquid phase occurs at 26–30 °C. Dissociation of $CO_2$-clathrate ($CO_2 \cdot 5\frac{3}{4}$ $H_2O$) occurs at 3–4 °C in the presence of liquid $CO_2$ and $CO_2$ vapor and total homogenization to the liquid phase occurs at approximately 320 °C. These phase transitions suggest that the fluid is $H_2O$–$CO_2$–"salt" with about 10 mol.% $CO_2$ and salinity of 11–12 wt.% NaCl equivalent. The depression of the $CO_2$ melting point from $-56.6$ °C to $-57$ °C suggests that the inclusions may contain as much as 0.5 mol.% $CH_4$ or $N_2$. The average size of these inclusions is 5 $\mu$m.

Sioux quartzite contains dominantly one-phase, aqueous liquid inclusions at room temperature (type 5). They occur in irregular patches (Fig. 3F), along oriented or unoriented (Fig. 3G) healed microfractures, and along grain boundaries (Fig. 3F, J). The latter define boundaries between original quartz grains and syntaxial rim cement. Some healed microfractures transect the rim cement/quartz grain boundary but rarely cross two adjacent quartz grains. Partially decrepitated fluid inclusions with vapor bubbles display $T_e$ of $-22$ °C and $T_m$ ice of $-5$ to $-10$ °C, suggesting that the fluids are NaCl–$H_2O$ with salinities of 8–14 wt.% NaCl equivalent. These inclusions average about 2–3 $\mu$m in size.

## Results

Decrepitation profiles, showing the percentage of the total number of decrepitations as a function

of temperature, for Westerly granite and Sioux quartzite are presented in Figs. 5A and 6A, respectively. Decrepitation events were recorded by visually monitoring fluid inclusions with a petrographic microscope and recording as the decrepitation temperature the temperature at which the inclusion exploded, or experienced an increase in $T_h$ as explained above. Acoustic emission profiles of Westerly granite and Sioux quartzite from the work of Johnson et al. (1978) are shown in Figs. 5B and 6B, respectively, for comparison. The total number of events recorded in our study for each decrepitation profile is on the order of $10^2$ as compared to $10^3$ to $10^5$ events for the acoustic emission work of Johnson et al. (1978). As noted above, however, we believe that the subpopulations of inclusions we have chosen for each sample are representative of the entire population in the samples. That is, the histograms we have constructed accurately represent the decrepitation profiles of the samples; more data would not change the shapes of the profiles, only the absolute values on the ordinate. In order to compare results from the two studies, each data set was normalized so that each fifty degree temperature interval of the histogram shows the percentage of the total number of events for the experiment that were recorded in that interval.

Decrepitation in Westerly granite begins at ~ 75° C, increases steadily and reaches a maximum at 275–300° C, and then decrease steadily to 400° C (Fig. 5A). A second peak occurs at 400–450° C and a small decrepitation peak also occurs at the quartz $\alpha$–$\beta$ transition temperature (573° C). None of the test inclusions survived temperatures higher high 573° C. Type (4) fluid inclusions, which contain $CO_2$, tend to decrepitate at the lowest temperatures, averaging 212° C (Fig. 5A; Table 1) and most decrepitate prior to homogenization. This results from the high pressures generated during heating of moderate to high density $CO_2$–$H_2O \pm$ salt fluids. Primary decrepitations from type (1) inclusions occur at an average temperature of 261° C, while secondary decrepitations occur at an average temperature of 479° C

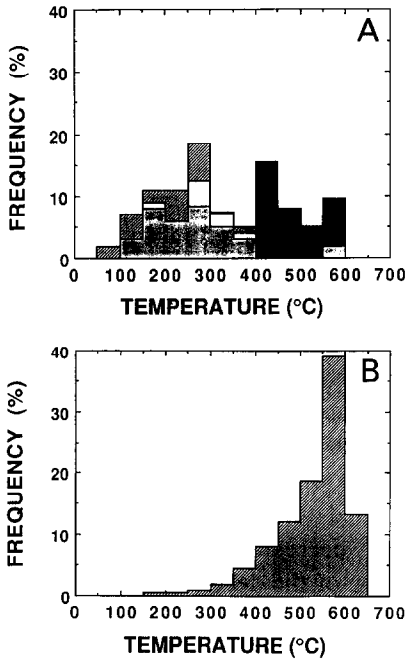


Fig. 5. A. Fluid inclusion decrepitation profile for Westerly granite. Dot pattern—Type (1), primary decrepitations; closed pattern—Type (1), secondary decrepitations; open pattern—Type (2); hatchured pattern—Type (4). B. Acoustic emission profile for Westerly granite, modified after Johnson et al. (1978). Both profiles have been normalized to 100 total events.

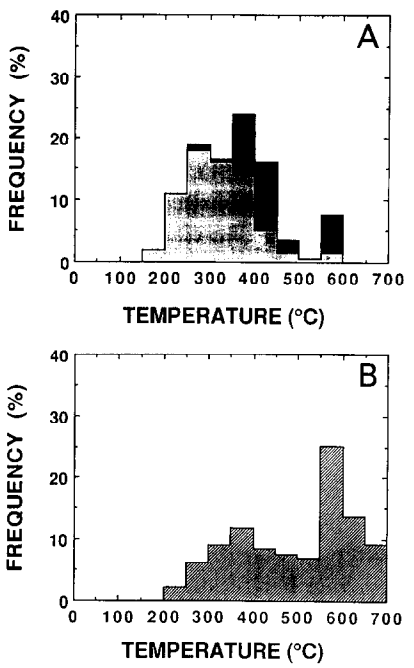


Fig. 6. A. Fluid inclusion decrepitation profile for Sioux quartzite. Dot pattern—primary decrepitations; closed pattern—secondary decrepitations. B. Acoustic emission profile for Sioux quartzite, modified after Johnson et al. (1978). Both profiles have been normalized to 100 total events.

(Fig. 5A; Table 1). Type (3) inclusions decrepitate at an average temperature of 288° C.

The acoustic emission profile for Westerly granite (Fig. 5B) differs significantly from the decrepitation profile described above. Acoustic emission commences at ~75° C and increases approximately exponentially to the $\alpha$–$\beta$ transition, after which the rate decreases rapidly. Nearly 40% of the emissions recorded by Johnson et al. (1978) occurred within ±25° C of the $\alpha$–$\beta$ transition.

Fluid inclusions in Sioux quartzite begin to decrepitate near 200° C (Table 1). The number of decrepitations increases abruptly with temperature and attains a broad maximum between 250° and 450° C, after which it drops rapidly to 500° C (Fig. 6A). As in Westerly granite, a small spike is recorded at the $\alpha$–$\beta$ transition and no test fluid inclusion survived temperatures above 573° C. Primary decrepitations occur at an average temperature of 321° C, while secondary decrepitations occur at an average temperature of 439° C (Fig. 6A; Table 1). The acoustic emission profile for Sioux quartzite (Fig. 6B) is very similar to the decrepitation profile. Acoustic emission is initiated at ~200° C, attains a broad maximum from 280–400° C, decays to a minimum around 550° C and then increases significantly at the $\alpha$–$\beta$ transition.

The increase in acoustic emission activity at approximately 573° C has been attributed to the large volume percent expansion of quartz near the $\alpha$–$\beta$ transition (Fig. 7). The volume increase causes significant intragranulur fracturing and microcrack propagation in both quartz and feldspar near 573° C (Johnson et al., 1978; Fredrich and Wong, 1986). A similar peak at the $\alpha$–$\beta$ transition is usually found during decrepitation studies as well (Burlinson et al., 1983; Hladky and Wilkins, 1987; Bodnar et al., 1989) and has been documented in a number of studies which use thermal decrepitation to release inclusion contents for analysis (Barker and Robinson, 1984). Bodnar et al. (1989) have suggested that decrepitation near the quartz $\alpha$–$\beta$ transition results from the pressure dependence of the transition temperature (Koster van Groos and Ter Heege, 1973; Van der Molen, 1981). The pressure on the walls of the

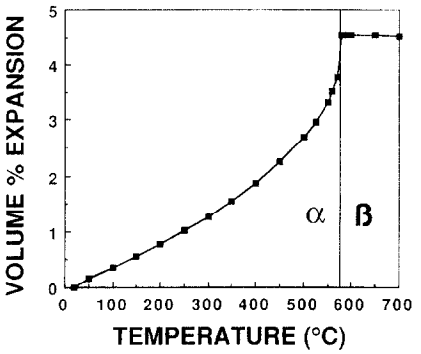


Fig. 7. Volume percent expansion of quartz as a function of temperature showing the large volume increase near the $\alpha$–$\beta$ transition. Data from Skinner (1966).

fluid inclusion may be several kilobars while the bulk of the quartz matrix is at a significantly lower pressure. The pressure gradient across the fluid inclusion wall causes the $\alpha$–$\beta$ transition to occur at significantly higher temperatures near the inclusion compared to further away, resulting in structural discontinuities in the crystal and increased stress in the matrix near the fluid inclusions.

## Discussion

Two important questions concerning decrepitation and acoustic emission analyses were posed earlier. Specifically, does fluid inclusion decrepitation contribute to acoustic emission profiles? If it does, what portion of the recorded events are from decrepitation and what portion are from thermoelastic stresses involving solid–solid interactions? In order to answer these questions, the energies associated with the two different events must be known. There is some question as to whether apparatus used to detect acoustic emissions will also record decrepitating fluid inclusions and whether some of the decrepitation events recorded in decrepitometry are related to thermoelastic effects. The two methods usually use different detection devices—a PZT transducer for acoustic emission studies and generally a sensitive microphone in decrepitation studies. Detection frequencies as low as 5 kHz and as high as 5 MHz have been reported for acoustic emission studies, while de-

crepitation studies detect events over the range 0.5–5 kHz. There is no *a priori* reason why fluid inclusion decrepitation events should not be recorded during acoustic emission measurement because both phenomena involve microfracturing of the sample, and the "size" of the fractures appears to be similar based on published results. The determining factor is the magnitude of the acoustic energy released during decrepitation and whether it is sufficient in some cases to be recorded in the 5kHz to 5 MHz range. We do not presently have an answer to this question, but it is the subject of continuing research and will be addressed in future communications.

Our goal in this preliminary phase of the study was simply to compare the decrepitation and acoustic emission profiles of Westerly granite and Sioux quartzite, and this we have accomplished. However, if we *assume* that decrepitating fluid inclusions are recorded during acoustic emission analyses and that the relative number of decrepitations recorded as a function of temperature is similar to that observed in this study, then we can speculate on the relative contribution of decrepitation to various portions of the acoustic emission profiles for the two rock types studied. With this assumption in mind, our observations suggest that decrepitating fluid inclusions contribute more to lower temperature portions of acoustic emission profiles of Westerly granite and Sioux quartzite than to higher temperature portions. For instance, 62% and 72% of the recorded decrepitations occur below 400 °C in Westerly granite and Sioux quartzite, respectively. This is primarily due to the predominance in both rocks of inclusions that are one-phase liquids at room temperature. Fluid inclusions of this type attain high internal pressures at relatively low temperatures. The $H_2O$–$CO_2$–"salt" inclusions in Westerly granite also attain high internal pressures at low temperatures and most of these fluid inclusions decrepitate before the homogenization temperature is reached (see Fig. 3H). Other rocks that contain lower density aqueous inclusions would be expected to display decrepitation profiles displaced significantly toward higher temperatures compared to those presented here for Westerly granite and Sioux quartzite.

Fluid inclusion decrepitation contributes more to the low temperature decrepitation profile of Sioux quartzite than that of Westerly granite. This results in part from the larger number of fluid inclusions per unit volume of Sioux quartzite compared to Westerly granite. Petrographic estimates of fluid inclusion abundances range from $10^7$ to $10^8$ inclusions/cm$^3$ in Westerly granite, and from $10^8$ to $10^9$ inclusions/cm$^3$ in Sioux quartzite. Thus, there is on the average an order of magnitude more fluid inclusions in a given volume of Sioux quartzite than in the same volume of Westerly granite.

Based on the similarities of the two profiles shown in Figs. 6A and 6B, it is possible that decrepitating fluid inclusions contribute significantly to the broad, low-temperature maximum present in the acoustic emission profile of Sioux quartzite (Fig. 6B). The low-temperature maximum on the decrepitation profile of Westerly granite is not resolved on the acoustic emission profile of Johnson et al. (1978) at the scale plotted in Fig. 5B. However, looking at their original data (Fig. 10 of Johnson et al., 1978) there is a small maximum centered on 175 °C, which may correspond to our maximum centered at 250 °C. Furthermore, the acoustic emission study of Yong and Wang (1980) indicates a steady increase in acoustic emission activity from a threshold temperature of 60–70 °C up to 120 °C, the upper temperature limit of their study. This is qualitatively consistent with our decrepitation data (Fig. 6A). Fluid inclusions in Sioux quartzite are more uniform in size, shape, density and composition than those in Westerly granite. These factors all contribute to the temperature at which a particular inclusion decrepitates at one atmosphere (see Bodnar et al., 1989) and it is, therefore, not surprising that a larger percentage of decrepitations in Sioux quartzite occur over a smaller temperature range than in Westerly granite.

A large percentage of intragranular fractures in quartz in samples heated to maximum temperatures which were below the $\alpha$–$\beta$ transition could be traced to decrepitated fluid inclusions (Figs. 3H, 3I, 4B and 4C). These fractures could be observed occasionally as they formed during heating tests to determine decrepitation profiles in this

study and, in a related study of the decrepitation behavior of fluid inclusions in quartz, Bodnar et al. (1989) observed fractures which originated at decrepitating inclusions and propagated outward into the host mineral. Often these fractures would continue to propagate until they reached the grain boundary. This same phenomenon is also commonly observed during standard microthermometric analyses of inclusions in a wide variety of rock and mineral samples (see Roedder, 1984).

*There is little doubt that, in general, decrepitating fluid inclusions cause the majority of intragranular fracturing in quartz when it is heated to temperatures below the $\alpha$–$\beta$ transition and that, in the present study, the intragranular fractures observed in both Westerly granite and Sioux quartzite originated in this manner.* The advantage we have in this study, compared to most acoustic emission studies, that allows us to reach this conclusion concerning the origin of intragranular fractures is that we are actually observing the sample during heating and are thus able to see the fractures as they originate, rather than examining the sample after the experiment is completed and having to infer the origin of the fractures. It should be noted that other mechanisms are usually cited in the acoustic emission literature as the cause of these intragranular fractures (S. Bauer, pers. commun., 1988), although direct observational evidence for these other mechanisms is not presented.

At temperatures near 573°C significant intragranular fracturing occurs without any recognizable relationship to the fluid inclusion distribution. Thus, most acoustic emissions in the vicinity of the quartz $\alpha$–$\beta$ transition appear to result from thermoelastic stresses between neighboring grains and may contain relatively little contribution from decrepitating fluid inclusions. However, Bodnar et al. (1989) and Barker and Robinson (1984) report that a larger portion of the total inclusion population decrepitates in the 20°C range that brackets the quartz $\alpha$–$\beta$ transition than in any other 20° range from room temperature to 600°C.

It was not possible to monitor individual fluid inclusions in feldspar in Westerly granite during this study. However, during SEM observation of previously heated samples, small microfractures were observed to emanate from fluid inclusions in feldspar (Fig. 4D) and nearly all healed intragranular microfractures in both plagioclase and microcline, which are decorated with tiny fluid inclusions, reopened during heating. Many of the large intragranular fractures in feldspar develop along cleavage directions during heating and are not related to the distribution of fluid inclusions. Wong (1982) also noted large numbers of microfractures emanating from "pores" in plagioclase in deformed samples of Westerly granite (see his Fig. 9) and reported that these fluid inclusions significantly affected the fracture characteristics of plagioclase.

Some workers (e.g., Heard and Page, 1982) have noted average deviations of measured rock properties which are much greater than the estimated precision. Other workers (e.g., Johnson et al., 1978) have recognized systematic variations in measured mechanical and transport properties between different samples of the same rock. These differences could not be explained by analytical error, and have been attributed to fabric (e.g., grain size) differences. Such inconsistencies may also be in part due to fracturing associated with decrepitation and to possible variations in numbers of fluid inclusions contained in different samples of the same rock. It should be noted that the distribution of fluid inclusions may be a function of the fabric of the rock as well. Johnson et al. (1978) found that samples of Sioux quartzite could be divided into two groups with distinctly different post-heating longitudinal-wave velocities, and that these groups came from two separate areas of the block of starting material. Samples with lower velocities at a given temperature also had lower threshold temperatures (near 200°C) for acoustic emission. Spatial differences in the abundance of fluid inclusions in the block of starting material could account for the differences in measured properties. Specifically, an increase in the abundance of one-phase, aqueous fluid inclusions in the low-velocity sample would cause increased microfracturing and thus decreased longitudinal-wave velocity at a given temperature. These inclusions could potentially cause an increase in acoustic emission activity at lower temperatures as well. This suggests that thin sections of samples should be prepared before acoustic emission studies are

conducted in order to determine the type and distribution of fluid inclusions in the samples.

## Acknowledgements

We are grateful to Brian Bonner and Mel Friedman for providing the samples of Westerly granite and Sioux quartzite, respectively, that were used in this study. Discussions with Rick Law and Geoff Lloyd were most helpful. We are indebted to Stephen Bauer and Herb Wang, whose incisive reviews significantly improved the manuscript, although we accept total responsibility for any errors or inconsistencies that remain. This study was supported by grants from the Earth Sciences Section of the National Science Foundation (NSF Grant EAR-8607356), the American Chemical Society Petroleum Research Fund (Grant No. 18861-G2), and by funds from the Department of the Interior's Mining and Mineral Resources Research Institute program administered by the Bureau of Mines under allotment grant G1164151.

## References

Atkinson, B.K., 1984. Subcritical crack growth in geological materials. J. Geophys. Res., 89: 4077–4114.

Atkinson, B.K., MacDonald, D. and Meredith, P.G., 1984. Acoustic response and fracture mechanics of granite subjected to thermal and stress cycling experiments. In: H.R. Hardy and F.W. Leighton (Editors), Proc. 3rd Int. Conf. on Acoustic Emission/Microseismic Activity in Geological Structures and Materials. Trans-Tech Pubs., Clausthal, pp. 5–18.

Barker, C. and Robinson, S.J., 1984. Thermal release of water from natural quartz. Am. Mineral., 69: 1078–1081.

Bauer, S.J. and Johnson, B., 1979. Effects of slow uniform heating on the physical properties of Westerly and Charcoal granites. Proc. 20th U.S. Symp. Rock Mech., Austin, Tex., pp. 7–19.

Birch, F., 1966. Compressibility; elastic constants. In: S.J. Clark (Editor), Handbook of Physical Constants. Geol. Soc. Am., Mem., 97.

Bodnar, R.J. and Bethke, P.M., 1984. Systematics of stretching of fluid inclusions. I. Fluorite and sphalerite at 1 atmosphere confining pressure. Econ. Geol., 79: 141–161.

Bodnar, R.J., Binns, P. and Hall, D.L., 1989. Synthetic fluid inclusions. VI. Quantitative evaluation of the decrepitation behavior of fluid inclusions in quartz at one atmosphere confining pressure. J. Metamorph. Geol., 7: 229–242.

Burlinson, K., 1989. Decrepitation as an aid to microthermometry (abstr.). 2nd Biennial Pan-Am. Conf. on Research on Fluid Inclusions, Progr. Abstr., 15.

Burlinson, K., Dubessy, J.C., Hladky, G. and Wilkins, R.W.T., 1983. The use of fluid inclusion decrepitometry to distinguish mineralized and barren quartz veins in the Aberfoyle tin–tungsten mine area, Tasmania. J. Geochem. Explor., 19: 319–333.

Burnham, C.W., Holloway, J.R. and Davis, N.F., 1969. Thermodynamic properties of water to 1,000 °C and 10,000 bars. Geol. Soc. Am., Spec. Pap., 132: 96 pp.

Carlson, S.C., Wang, H.F., Kowallis, B.J., Bonner, B.P. and Heard, H.C., 1986. Thermal stress microfracturing of three granites. Eos, Trans. Am. Geophys. Union, 67: 373.

Dunning, J.D., Petrovski, D., Schuyler, J. and Owens, A., 1984. The effects of aqueous chemical environments on crack propagation in quartz. J. Geophys. Res., 89: 4115–4123.

Durham, W.B. and Abey, A.E., 1981. The effect of pressure and temperature on the thermal properties of a salt and a quartz monzonite. Proc. U.S. Symp. Rock Mech., 22: 79–84.

Fredrich, J.T. and Wong, T.F., 1986. Micromechanics of thermally induced cracking in three crustal rocks. J. Geophys. Res., 91: 12,743–12,764.

Friedman, M. and Bur, T.R., 1974. Investigation of the relations among residual strain, fabric, fracture, and ultrasonic attenuation and velocity in rocks. Int. J. Rock. Mech. Min. Sci. and Geomech. Abstr., 11: 221–234.

Friedman, M. and Johnson, B., 1978. Thermal cracks in unconfined Sioux quartzite. Proc. U.S. Symp. Rock Mech., 19: 423–430.

Gratier, J.P. and Jenatton, L., 1984. Deformation by solution-deposition, and re-equilibration of fluid inclusions in crystals depending on temperature, internal pressure and stress. J. Struct. Geol., 6: 189–200.

Hadley, K., 1976. Comparison of calculated and observed crack densities and seismic velocities in Westerly granite. J. Geophys. Res., 81: 3484–3494.

Heard, H.C., 1980. Thermal expansion and inferred permeability of Climax quartz monzonite to 300 °C and 27.6 MPa. Int. J. Rock Mech. Min. Sci., 17: 289–296.

Heard, H.C. and Page, L., 1982. Elastic moduli, thermal expansion, and inferred permeability of two granites to 350 °C and 55 MPa. J. Geophys. Res., 87: 9340–9348.

Hladky, G. and Wilkins, W., 1987. A new approach to fluid inclusion decrepitometry-practice. Chem. Geol., 61: 37–45.

Johnson, B., Gangi, A.F. and Handin, J., 1978. Thermal cracking of rocks subjected to slow, uniform temperature change. Proc. U.S. Symp. Rock Mech., 19: 259–267.

Koster Van Groos, A.F. and Ter Heege, J.P., 1973. The high-low quartz transitions up to 10 kilobars pressure. J. Geol., 81: 717–723.

Kurita, K. and Fujii, N., 1979. Stress memory of crystalline rocks in acoustic emission. Geophys. Res. Lett., 6: 9–12.

Leroy, J., 1979. Contribution à l'étalonnage de la pression interne des inclusions fluides lors de leur décrépitation. Bull. Soc. Fr. Minéral. Cristallogr., 102: 584–593.

Meredith, P.G. and Atkinson, B.K., 1985. Fracture toughness and subcritical crack growth during high temperature tensile deformation of Westerly granite and Black gabbro. Phys. Earth Planet. Inter., 39: 33–51.

Morrow, C., Lockner, D., Moore, D. and Byerlee, J., 1981. Permeability of granite in a temperature gradient. J. Geophys. Res., 86: 3002–3008.

Olhoeft, G.R., 1981. Electrical properties of granite with implications for the lower crust. J. Geophys. Res., 86: 931–936.

Peach, P.A., 1949. The decrepitation geothermometer. Am. Mineral., 34: 413–421.

Poland, E.L., 1982. Stretching of fluid inclusions in fluorite at confining pressures up to 1 kilobar. M.S. Thesis, Univ. of California, Berkeley, Calif., 90 pp. (unpublished).

Potter, J.M., 1978. Experimental permeability studies at elevated temperature and pressure of granitic rocks. Los Alamos Scientific Laboratory, Rep. LA-7224-T, May: 101 pp.

Roedder, E., 1984. Fluid Inclusions. Rev. Mineral, Mineral. Soc. Am., 12: 644 pp.

Scott, H.S., 1948. The decrepitation method applied to minerals with fluid inclusions. Econ. Geol., 43: 637–645.

Simmons, G. and Cooper, H.W., 1978. Thermal cycling cracks in three igneous rocks. Int. J. Rock Mech. Min. Sci., 15: 145–148.

Skinner, B.J., 1966. Thermal expansion. In: S.J. Clark (Editor), Handbook of Physical Constants. Geol. Soc. Am., Mem., 97.

Smith, F.G., 1950. A method of determining the direction of flow of hydrothermal solutions. Econ. Geol., 45: 62–69.

Summers, R., Winkler, K. and Byerlee, J., 1978. Permeability changes during the flow of water through Westerly granite at temperatures of 100°–400°C. J. Geophys. Res., 83: 339–344.

Swanson, P.L., 1984. Subcritical crack growth and other time- and environment-dependent behavior in crustal rocks. J. Geophys. Res., 89: 4137–4152.

Trimmer, D., Bonner, B., Heard, H.C. and Duba, A., 1980. Effect of pressure and stress on water transport in intact and fractured gabbro and granite. J. Geophys. Res., 85: 7059–7071.

Tugarinov, A.I. and Naumov, V.B., 1970. Dependence of the decrepitation temperature of minerals on the composition of their gas–liquid inclusions and hardness. Dokl. Akad. Nauk SSSR, 195: 112–114.

Ulrich, M.R. and Bodnar, R.J., 1988. Systematics of stretching of fluid inclusions, II. Barite at one atmosphere confining pressure. Econ. Geol., 83: 1037–146.

Van der Molen, I., 1981. The shift of the $\alpha/\beta$ transition temperature of quartz associated with the thermal expansion of granite at high pressure. Tectonophysics, 73: 323–342.

Walsh, J. and Decker, E.R., 1966. Effect of pressure and saturating fluid on the thermal conductivity of compact rock. J. Geophys. Res., 71: 3053–3061.

Wang, H.F. and Heard, H.C., 1985. Prediction of elastic moduli via crack density in pressurized and thermally stressed rock. J. Geophys. Res., 90: 10342–10350.

Wang, H.F., Bonner, B.P., Carlson, S.R., Kowallis, B.J. and Heard, H.C., 1989. Thermal stress cracking in granite. J. Geophys. Res. 94: 1745–1758.

Werre, R.W., Jr., Bodnar, R.J., Bethke, P.M. and Barton, P.B., Jr., 1979. A novel gas-flow fluid inclusion heating/freezing stage (abstr.). Geol. Soc. Am., Abstr. Progr., 11: 539.

Wong, T.F., 1982. Micromechanics of faulting in Westerly granite. Int. J. Rock Mech. Min. Sci., 19: 49–54.

Wong, T.F. and Brace, W.F., 1979. Thermal expansion of rocks: some measurements at high pressure. Tectonophysics, 57: 95–117.

Yong, C. and Wang, C., 1980. Thermally induced acoustic emission in Westerly granite. Geophys. Res. Lett., 7: 1089–1092.